

# The method of the apparent vertical applied to pendulum dynamics



**Héctor A. Múnera and Héctor R. Maya**

*International Centre for Physics (CIF Centro Internacional de Física),  
A. P. 4948, Bogotá, Colombia.*

*Department of Physics, Universidad de Córdoba, Montería, Colombia  
and Department of Physics, Universidad Nacional de Colombia, Bogotá, Colombia.*

**E-mail:** hmunera@hotmail.com

(Received 15 November 2010; accepted 10 January 2011)

## Abstract

The paper describes the geometrical method of the apparent vertical (MAV for short) for the solution of a large class of problems in elementary classical mechanics: perturbation of a dynamical system by a constant or nearly constant force, not necessarily small. The basic idea is to rotate the system of coordinates so that the  $z$ -axis coincides with an “apparent” acceleration of gravity. The solution in the rotated system is simpler than in the unrotated coordinates, and it is usually known. The methodology is illustrated with a spherical pendulum in a uniform field of force, where the standard solution in terms of elliptic functions is directly applicable in the rotated system of coordinates. The trajectory of the bob in the usual coordinates attached to the laboratory is obtained by a straightforward rotation of coordinates, thus allowing calculation of the observable parameters: amplitude, period, and plane of oscillation of the pendulum.

**Keywords:** spherical pendulum dynamics, perturbed dynamical systems, geometrical solution of equations of motion.

## Resumen

En el documento se describe el método geométrico de la vertical aparente (para abreviar, MAV, por las iniciales en inglés) para la solución de una gran clase de problemas en la mecánica clásica elemental: la perturbación de un sistema dinámico de una fuerza constante o casi constante, no necesariamente pequeña. La idea básica consiste en hacer girar el sistema de coordenadas de modo que el eje  $z$  coincide con una “aparente” aceleración de la gravedad. La solución en el sistema de rotación es más sencillo que en las coordenadas sin rotar, y es generalmente conocido. La metodología se ilustra con un péndulo esférico en un campo uniforme de fuerza, donde la solución estándar en términos de funciones elípticas es directamente aplicable en el sistema de coordenadas asociado con la vertical aparente. La trayectoria del movimiento en las coordenadas habituales ancladas al laboratorio se obtiene mediante una sencilla rotación de coordenadas, lo que permite el cálculo de los parámetros observables: amplitud, periodo, y el plano de oscilación del péndulo.

**Palabras clave:** dinámica del péndulo esférico, sistemas dinámicos perturbados, solución geométrica de las ecuaciones de movimiento.

**PACS:** 45.30.+s, 45.20.-d

**ISSN 1870-9095**

## I. INTRODUCTION

Problems in elementary classical dynamics are represented by an equation of motion, usually referred to a system of coordinates  $OXYZ$ , selected so that the  $z$ -axis coincides with the local direction of terrestrial gravitational attraction  $\mathbf{g}$ . Let us assume that the solution to a given problem is already known. What happens if we introduce an additional force  $\mathbf{F}$ , approximately constant, or slowly varying in time? The solution to the new equation of motion is usually known from the theory of differential equations. Here we want to introduce an alternative geometrical method, which is entirely equivalent to the usual mathematical procedure, that we call the method of the apparent vertical (MAV for short).

The MAV may be applied to any dynamical system subject to a constant or nearly constant (not necessarily small) perturbation, but the method is illustrated here with the spherical pendulum perturbed by the gravitational fields of the sun and the moon, problem that is of some current interest. [1, 2, 3, 4, 5, 6, 7].

The basic idea of the MAV is to make a rotation of coordinates to a new system  $OX^*Y^*Z^*$ , where the direction of the rotated  $z^*$ -axis coincides with an apparent gravity  $\mathbf{g}^*$ . The rotation of coordinates used in the MAV is reminiscent of the graphical algorithms use to define the addition of bivectors in geometric algebra (recall that an axial vector in the usual vector algebra is the same as a bivector in geometric algebra, [8, 9]).

## II. THE METHOD OF THE APPARENT VERTICAL

Rather than entering into explanations in abstract, the method of the apparent vertical (MAV) is introduced with an example. Consider an ideal pendulum of mass  $m$  suspended from an inextensible and massless cord of length  $L$  in a laboratory rigidly attached to our earth. The support is an ideal fixed point C, located at the origin of a Cartesian system of coordinates  $S = (x, y, z)$ , with the  $z$ -axis pointing in the same direction as the local vertical  $\mathbf{g} = g\mathbf{k}$  defined by the plumb line, i.e.  $\mathbf{g}$  is the vector sum of earth's gravitational acceleration plus the centrifugal acceleration associated with earth's rotation. As usual,  $\mathbf{i}, \mathbf{j}, \mathbf{k}$  are the unit vectors of a Cartesian frame of reference. The pendulum is released at  $t = 0$  from  $x = q = L \sin \theta_0, y = 0, z = h = L \cos \theta_0$  as shown in figure 1A. The position of the bob at any time  $t$  is given by  $\mathbf{r} = x\mathbf{i} + y\mathbf{j} + z\mathbf{k}$ , and its equation of motion is

$$m \frac{d^2 \mathbf{r}}{dt^2} = m\mathbf{A} + m\mathbf{g} + \mathbf{T} = m\mathbf{g}^* + \mathbf{T}, \quad (1)$$

where constant force  $\mathbf{F} = m\mathbf{A} = m(A_x\mathbf{i} + A_y\mathbf{j} + A_z\mathbf{k})$  continuously acts upon the bob, say a constant wind, the time dependent tension is  $\mathbf{T}$ , and the apparent gravity  $\mathbf{g}^*$  is,

$$\mathbf{g}^* = \mathbf{A} + \mathbf{g} = A_x\mathbf{i} + A_y\mathbf{j} + (A_z + g)\mathbf{k}. \quad (2)$$

The last expression on the right-hand side of Eq. (1) means that the dynamics of the pendulum in a system with apparent gravity  $\mathbf{g}^*$  is the same as the usual dynamics of a pendulum subject to gravity  $\mathbf{g}$  only. We just need to rotate the system of coordinates  $S = (x, y, z)$  in an appropriate manner to get  $S^* = (x^*, y^*, z^*)$  so that the new  $z^*$ -axis is aligned with the direction of  $\mathbf{g}^*$ .

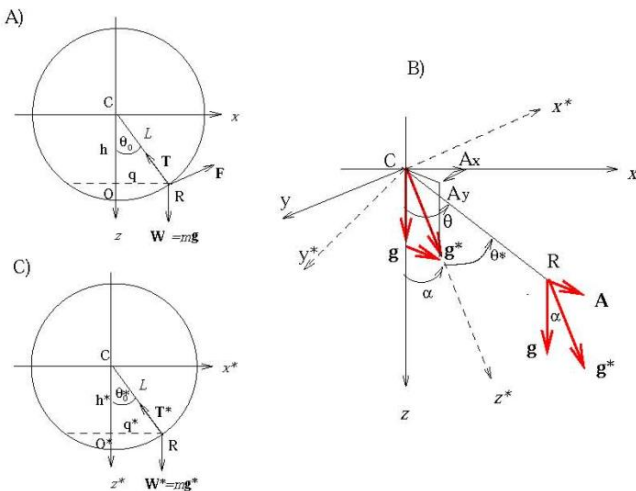


**FIGURE 1.** Plane of oscillation, force diagrams, and rotation of coordinates in 3D space. A) Usual coordinates in the laboratory. The  $z$ -axis is aligned with the local vertical  $\mathbf{g}$ . The  $y$ -axis points out of page, and  $\mathbf{F}$  may have components in  $y$ . Point O (often used as a reference) is the projection of support C onto the laboratory

horizontal floor. Line CR is in the  $zx$ -plane. B) Rotation of coordinates to align the  $z^*$ -axis with  $\mathbf{g}^*$ , and to include line CR in the  $z^*x^*$ -plane. In general angles  $\alpha, \theta,$  and  $\theta^*$  are in different planes. C) At the moment of release, the pendulum is in the  $z^*x^*$ -plane.

We denote all variables in the apparent vertical coordinates by an asterisk added to the corresponding concept in the unrotated laboratory coordinates. Formally, in the rotated coordinates  $S^*$  the position of the bob at any time  $t$  is given by  $\mathbf{r}^* = x^*\mathbf{i}^* + y^*\mathbf{j}^* + z^*\mathbf{k}^*$  (evidently  $\mathbf{r} = \mathbf{r}^*$ ). The new equation of motion is

$$m \frac{d^2 \mathbf{r}^*}{dt^2} = m\mathbf{g}^* + \mathbf{T}^*. \quad (3)$$

For convenience in the description of the problem in  $S^*$ , we have imposed the further condition that the physical line CR, defined by the initial release of the bob, is in the same geometry in both systems of coordinates  $S$  and  $S^*$  (compare figures 1A and 1C). From Eq. 3 it follows that all standard solutions for the planar, spherical and physical pendulums are applicable in  $S^*$  provided that we write  $\mathbf{g}^*$  instead of  $\mathbf{g}$ . Obviously, force  $\mathbf{F}$  does not appear any longer.

Note that the *apparent* acceleration of gravity  $\mathbf{g}^*$  defined by Eq. (2) is not the same as the *effective or equivalent* acceleration of gravity defined in the context of Einstein's principle of equivalence (A has a different sign), see, for instance, [10]. It is stressed that in the MAV there is one frame of reference (the laboratory) only, but two systems of coordinates  $S$  and  $S^*$  with a common origin.

## III. ROTATION OF COORDINATES WHEN $A_y=0$

Let  $\alpha$  be the angle between the usual vertical  $\mathbf{g}$  and the apparent vertical  $\mathbf{g}^*$  given by

$$\cos \alpha = \frac{\mathbf{g} \cdot \mathbf{g}^*}{g g^*} = \frac{A_z + g}{g^*}. \quad (4)$$

The magnitude of the apparent gravity is

$$g^* = \sqrt{A_x^2 + A_y^2 + (A_z + g)^2} = g \sqrt{k_x^2 + k_y^2 + 1 + k_z^2}, \quad (5)$$

where the reduced components of acceleration  $\mathbf{A}$  are  $k_j = A_j/g$  for  $j = x, y, z$ .

Consider now the elementary text-book problem of a pendulum released at time  $t = 0$  from  $x = q, y = 0, z = h$ , with  $\mathbf{F} = 0$ . The bob moves on a plane of oscillation  $P$  defined by the two forces acting upon the pendulum — weight  $\mathbf{W} = m\mathbf{g}$ , and tension  $\mathbf{T}$ . In figure 1A the plane  $P$  coincides with the  $zx$ -plane, i.e. there are no components of force transversal to plane  $P$ . In this case, both  $\alpha$  and  $\mathbf{g}^*$  are contained in the same plane  $P$ , as shown in figure 2 for the case  $A_x > 0$  and  $A_z > 0$ .

In Fig. 2 it is evident by direct inspection that the angular amplitude of oscillation is  $\theta_0^* = \theta_0 - \alpha$ .

If  $\alpha < \theta_0$ , then  $q^* = L \theta_0^* \sin \theta_0^* < q$ ; if  $\theta_0 = \alpha$ , then  $q^* = 0$ , and the pendulum remains at rest; and, if  $\alpha > \theta_0$  the pendulum behaves as if released from the left side (i.e. the negative  $x^*$ -axis), and  $q^*$  may be smaller or larger

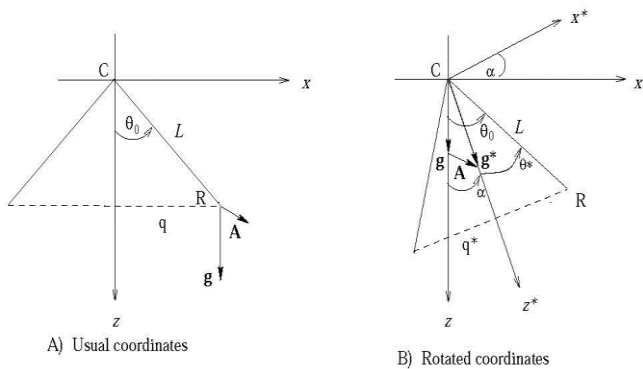


**FIGURE 2.** Two dimensional (2D) rotation of coordinates when  $A_y = 0$ . A) Usual 2D-diagram of force. B) Rotation around the  $y$ -axis through angle  $\alpha$  aligns the  $z$ -axis with the apparent vertical  $\mathbf{g}^*$ . This example corresponds to  $A_x > 0$ ,  $A_z > 0$ . The angular amplitude of oscillation is  $\theta_0^* = \theta_0 - \alpha$ . If  $\alpha < \theta_0$  then  $q^* = L \sin \theta_0^* < q$ ; if  $\alpha = \theta_0$ ,  $q^* = 0$ , and the pendulum remains at rest, and if  $\alpha > \theta_0$  the pendulum behaves as if released from the left side.

than  $q$  depending upon the magnitude of acceleration  $A_x$ . Similar considerations apply for  $A_x < 0$ .

For an arbitrary initial amplitude of release  $q^*$  or  $\theta_0^*$ , the standard solution for a pendulum released from rest is [11, 12, 13]

$$x^* = L \sin[\theta^*(t)], \quad y^* = 0, \quad z^* = L \cos[\theta^*(t)], \quad (6)$$

$$\theta^*(t) = 2 \arcsin \left[ \sqrt{n} \operatorname{sn} \left[ \omega_0^*(t - t_0); n \right] \right], \quad (7)$$

$$\text{where } n = \sin^2[\theta_0^*/2], \text{ and } \omega_0^{*2} = g^*/L.$$

The parameter  $n$  is the module of the Jacobi elliptic function  $\operatorname{sn}$ . As usual, the period of oscillation of the pendulum  $\tau$  is obtained from the period of the Jacobi elliptic function  $\operatorname{sn}$

$$\tau_{\text{Jacobi}} = \omega_0^* \tau = 4K n, \quad (8)$$

where  $K$  is the elliptic integral of the first kind

$$K n = \int_0^{\pi/2} \frac{dq}{\sqrt{1 - n \sin^2 q}}. \quad (9)$$

Then,

The method of the apparent vertical applied to pendulum dynamics

$$\tau = \frac{4K n}{\omega_0^*} = 4K n \sqrt{\frac{L}{g^*}} = \frac{\tau_0}{\sqrt{k_x^2 + 1 + k_z^2}}, \quad (10)$$

where  $\tau_0$  is the period of the pendulum when  $\mathbf{F} = 0$ , given by

$$\tau_0 = \frac{4K n}{\omega_0} = 4K(n) \sqrt{\frac{L}{g}} \text{ for arbitrary } \theta_0, \quad (11)$$

$$\tau_0 \approx \frac{2\pi}{\omega_0} = 2\pi \sqrt{L/g} \text{ for small } \theta_0. \quad (12)$$

Evidently,  $\tau < \tau_0$  if  $A_z > 0$  any  $A_x$ , i.e. if force  $\mathbf{F}$  pulls downwards. However, if  $A_z < 0$  there is no definitive trend.

The trajectory of the pendulum in laboratory coordinates  $S$  is easily obtained from Eq. (6) by a simple rotation  $R_\alpha$  applied to the position vector  $\mathbf{r}^* = (x^*, y^*, z^*)$  in the rotated system  $S^*$ :

$$\begin{pmatrix} x \\ y \\ z \end{pmatrix} = \begin{pmatrix} \cos \alpha & 0 & \sin \alpha \\ 0 & 1 & 0 \\ -\sin \alpha & 0 & \cos \alpha \end{pmatrix} \begin{pmatrix} x^* \\ y^* \\ z^* \end{pmatrix} = R_\alpha \begin{pmatrix} x^* \\ y^* \\ z^* \end{pmatrix}. \quad (13)$$

### Example 1. Vertical force $\mathbf{F}$ .

A pendulum is released from rest with initial conditions  $\theta = \theta_0$ ,  $x = L \sin \theta_0$ ,  $y = 0$ ,  $z = \cos \theta_0$ ,  $\dot{x} = 0$ ,  $\dot{y} = 0$ ,  $\dot{z} = 0$  in the presence of force  $\mathbf{F}$  characterized by  $k_x = 0$ ,  $k_y = 0$ ,  $k_z \neq 0$ , and  $k_z \neq -1$ . This is the trivial case of an apparent vertical acceleration with same direction as  $g$ , but different magnitude  $g^* = g(1 + k_z)$ . Eq. 10 reduces to  $\tau = \tau_0 / \sqrt{\operatorname{abs}(1 + k_z)}$ , so that  $\tau < \tau_0$  if  $k_z > 0$  and  $k_z < -2$ , but  $\tau > \tau_0$  if  $-2 < k_z < 0$ . Neither the amplitude, nor the plane of oscillation of the pendulum are modified by a vertical force  $\mathbf{F}$ .

### Example 2. Longitudinal force $\mathbf{F}$ .

Consider a pendulum released as in previous example in the presence of force  $\mathbf{F}$  producing acceleration parallel to the direction of oscillation, i.e.  $k_x \neq 0$ ,  $k_y = 0$ ,  $k_z = 0$ , leading to  $g^* > g$ . If  $k_x > 0$  there is a counter-clockwise rotation through angle  $\alpha$  given by

$$g^* = g \sqrt{1 + k_x^2}, \quad \cos \alpha = \frac{1}{\sqrt{1 + k_x^2}}. \quad (14)$$

If  $k_x < 0$  the rotation is clockwise. Substituting the explicit values for  $x^*$ ,  $y^*$ ,  $z^*$  given by Eq. 6 into Eq. 13,

$$\begin{aligned} x &= L \cos \alpha \sin \theta^*(t) + L \sin \alpha \cos \theta^*(t), \\ x &= L \sin[\theta^*(t) + \alpha], \\ y &= y^* = 0, \\ z &= -L \sin \alpha \sin \theta^*(t) + L \cos \alpha \cos \theta^*(t), \end{aligned} \quad (15)$$

$$z = L \cos[\theta^*(t) + \alpha].$$

Previous equations mean that in the usual laboratory coordinates a longitudinal force induces a phase angle  $\alpha$ , that is not present in the elementary case.

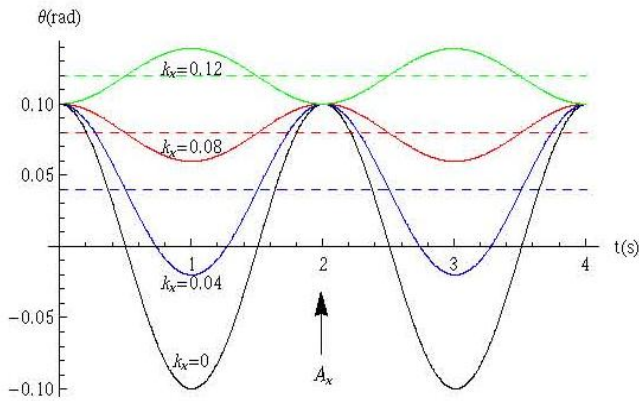


**FIGURE 3.** Angular position  $\theta$  as a function of time  $t$  for different values of  $k_x > 0$ . It also shows the values of the corresponding angles  $\alpha$  in dashed lines. The arrow indicates the direction of  $A_x$ .

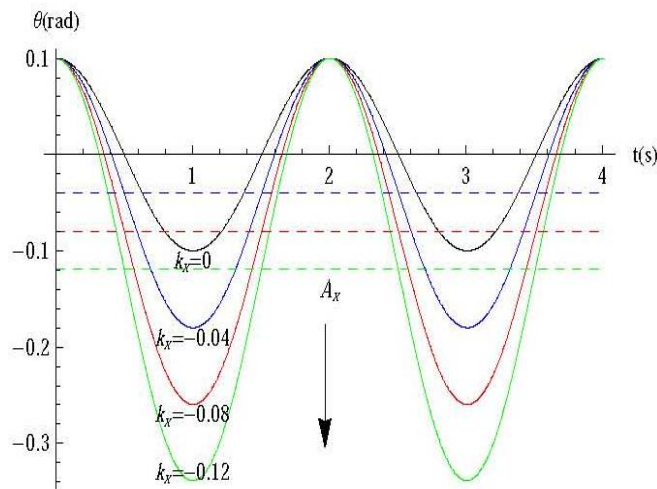


**FIGURE 4.** Angular position  $\theta$  as a function of time  $t$  for different values of  $k_x < 0$ . Dashes lines and arrow as in figure 3.

Fig. 3 shows the angular position  $\theta$  as function of time, for  $\theta_0 = 0.1 \text{ rad}$ ,  $L = 1 \text{ m}$ ,  $g = 9.8 \text{ m/s}^2$  and for different values of  $k_x$ . The curve  $k_x = 0$  is the elementary solution in the presence of terrestrial gravity only. When  $k_x > 0$  the bob oscillates with amplitude  $\theta_0 - \alpha$  around the *apparent* vertical, that in the graph corresponds to horizontal dashed lines for each  $k_x$ . Note that in the laboratory the amplitude decreases as  $k_x$  increases, until the pendulum remains at rest for  $k_x = \tan \theta_0$ . For large magnitudes of  $\mathbf{F}$ ,  $k_x > \tan \theta_0$ , the amplitude of the oscillation steadily increases.

The roots  $\theta = 0$  represent the successive passages of the pendulum through the local vertical. The time difference between two consecutive passages corresponds to *one half* period  $\tau_{1/2}$ . It is evident from Fig. 3 that the time taken for half a period in the left-region (i.e. negative  $\theta$ ) is longer than in the right-region (or positive  $\theta$ ), then  $\tau_{1/2\text{-left}} < \tau_{1/2\text{-right}}$  for  $k_x > 0$ ; the opposite holds for  $k_x < 0$  (see figure 4). In both cases the *full* period remains approximately constant:  $\tau_{1/2\text{-left}} + \tau_{1/2\text{-right}} = \tau$ .

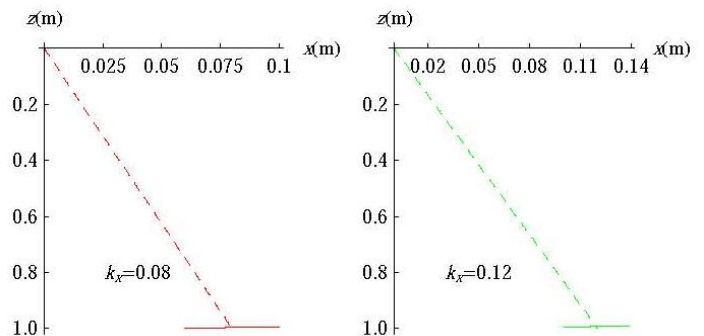
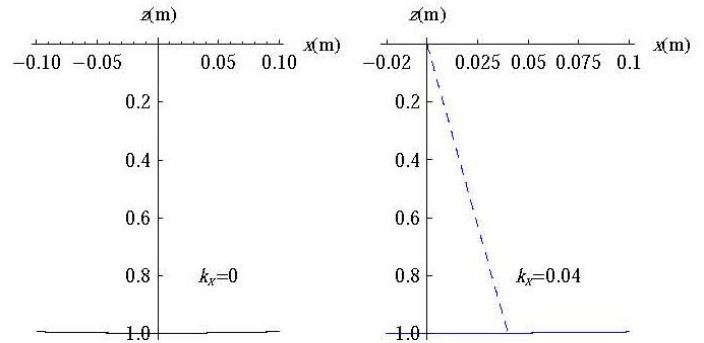


**FIGURE 5.** Trajectory in the  $zx$ -plane, for  $\theta_0 > 0$  and  $k_x > 0$ , values of  $k_x$  as in Fig. 3. The direction of  $A_x$  is given by the arrow.

Figs. 5 and 6 respectively show the trajectories in the  $zx$ -plane for the same values of  $k_x$  shown in Fig. 3 and 4, where the apparent vertical for each  $k_x$  is plotted as a dashed line. Note that amplitude and period are symmetrical with respect of the apparent vertical, but are asymmetrical with reference to the local, or laboratory, vertical. The shorter half-period on the left (right) side is evident from Fig. 3 and 5 (Figs. 4 and 6 respectively).

The period of oscillation  $\tau$  in the presence of a longitudinal force is shorter than the usual period  $\tau_0$  in the absence of  $\mathbf{F}$ :

$$\tau = \frac{\tau_0}{\sqrt{1+k_x^2}} \approx \tau_0 \left(1 - \frac{k_x^2}{4}\right). \quad (16)$$

Summarizing, a longitudinal  $\mathbf{F}$  shortens the period of oscillation and modifies the amplitude of oscillation in the laboratory, but the plane of oscillation of the ideal pendulum remains the same.

#### IV. GENERAL ROTATION FROM S-TO S\*-COORDINATES

In the general case  $A_y \neq 0$ , the plane  $P^*$  (or  $z^*x^*$ -plane) is defined by  $g^*$  and  $T^*$  when  $t = 0$ , and does not coincide with the  $zx$ -plane. Line CR is a physical connection between the point of suspension C and the position of the bob R at the instant of release, so that CR is the intercept between planes  $P$  and  $P^*$ . The rotation to transform from  $S$  to  $S^*$  hinges around line CR. Three successive operations are required: (1) Rotate the system of coordinates  $S$ , through angle  $\theta_0$  so that the  $z$ -axis coincides with CR; (2) Rotate the plane of oscillation  $P$  through angle  $\psi$  to the new orientation  $P^*$ ; (3) Rotate back through angle  $\theta_0^*$  so that the  $z^*$ -axis coincides with  $g^*$ , thus obtaining system of coordinates  $S^*$ .

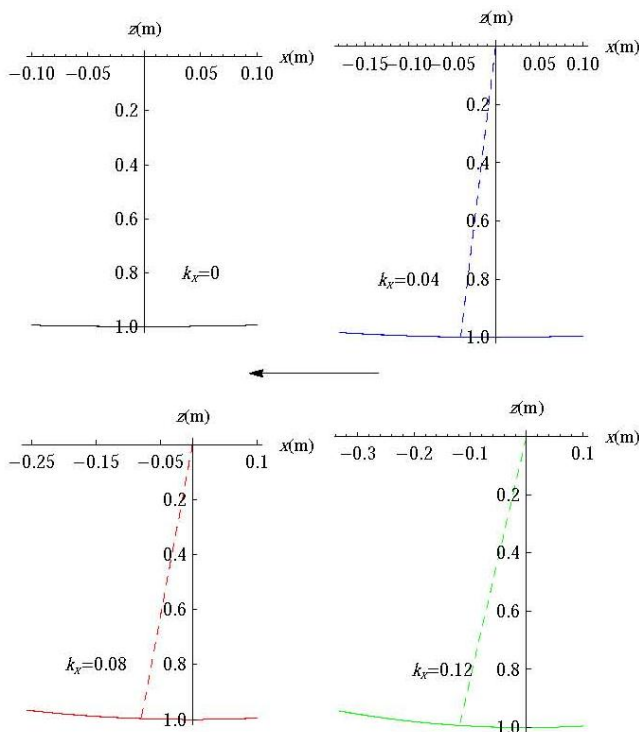


**FIGURE 6.** Trajectory in the  $zx$ -plane, for  $\theta_0 > 0$  and  $k_x < 0$ , for values of  $k_x$  in Figure 4. The arrow is the direction of  $A_x$ .

Note that the single rotation discussed in previous section is the special case  $\psi = 0$ , so that there is no change of orientation in the second rotation. Hence,  $\alpha = \theta_0 - \theta_0^*$  is produced by rotations 1 and 3. Now for the details of the general case (see Fig. 7):

(1) Let  $t = i \sin \theta_0 + k \cos \theta_0$  be a unit vector along CR, with direction opposite to the tension  $\mathbf{T}$  acting on the bob. A counter-clockwise rotation through angle  $\theta_0$  around the  $y$ -axis aligns the  $z$ -axis with unit vector  $\mathbf{t}$ , i.e. with the pendulum at the instant of release. Let us call this intermediate system  $S' = x'y'z'$ . The transformation is described by

The method of the apparent vertical applied to pendulum dynamics

$$\begin{bmatrix} x' \\ y' \\ z' \end{bmatrix} = R_1 \begin{bmatrix} x \\ y \\ z \end{bmatrix}; R_1 = \begin{bmatrix} \cos \theta_0 & 0 & -\sin \theta_0 \\ 0 & 1 & 0 \\ \sin \theta_0 & 0 & \cos \theta_0 \end{bmatrix}. \quad (17)$$

(2) The second rotation is through angle  $\psi$  –the angle between the normals to the  $zx$ - and  $z^*x^*$ -planes. Evidently, unit vector  $\mathbf{j}'$  is normal to the usual oscillation plane  $P$ . The normal vector  $\mathbf{N}$  to the oscillation plane  $P$  is  $\mathbf{N} = (g^* \times t) / g^*$ :

$$\mathbf{N} = \frac{1}{g^*} \{ \mathbf{i} A_y \cos \theta_0 + \mathbf{j} [ A_z + g \sin \theta_0 - A_x \cos \theta_0 ] - \mathbf{k} A_y \sin \theta_0 \}. \quad (18)$$

and its magnitude  $N$  is

$$N = \frac{g}{g^*} \sqrt{k_y^2 + [ 1 + k_z \sin \theta_0 - k_x \cos \theta_0 ]^2}. \quad (19)$$

Note the axial-vector  $\mathbf{N}$  is formed by unit vectors, but its magnitude is not 1. A rotation around the  $z'$ -axis through angle  $\psi$  brings the  $x'$ -axis onto the oscillation plane  $P^*$ . This intermediate system of coordinates is  $S'' = x''y''z''$ . Angle  $\psi$  is contained in the  $x'y'$ -plane (proof omitted) and is given by

$$\cos \psi = \frac{\mathbf{N} \cdot \mathbf{j}'}{N} = \frac{g}{Ng^*} (1 + k_z) \sin \theta_0 - k_x \cos \theta_0.$$

After this rotation the  $x''$ - and the  $z''$ -axes are contained in  $P^*$ , while the  $y''$ -axis is perpendicular to  $P^*$  (see Fig. 7). Formally, the second rotation is given by

$$\begin{bmatrix} x'' \\ y'' \\ z'' \end{bmatrix} = R_2 \begin{bmatrix} x' \\ y' \\ z' \end{bmatrix}; R_2 = \begin{bmatrix} \cos \psi & -\sin \psi & 0 \\ \sin \psi & \cos \psi & 0 \\ 0 & 0 & 1 \end{bmatrix}, \quad (20)$$

(3) The third rotation aligns the  $z''$ -axis with the effective vertical  $g^*$ . This requires a clockwise rotation through angle  $\theta_0^*$  around the  $y''$ -axis, given by

$$\begin{bmatrix} x^* \\ y^* \\ z^* \end{bmatrix} = R_3 \begin{bmatrix} x'' \\ y'' \\ z'' \end{bmatrix}; R_3 = \begin{bmatrix} \cos \theta_0^* & 0 & \sin \theta_0^* \\ 0 & 1 & 0 \\ -\sin \theta_0^* & 0 & \cos \theta_0^* \end{bmatrix}, \quad (21)$$

where angle  $\theta_0^*$  is defined by the direction of CR and vector  $g^*$  (see figures 1B and 1C) so that

$$\cos \theta_0^* = \frac{\mathbf{t} \cdot \mathbf{g}^*}{g^*} = \frac{g}{g^*} [ k_x \sin \theta_0 + 1 + k_z \cos \theta_0 ]. \quad (22)$$

Since the behavior of the pendulum is observed in the laboratory, we need the opposite transformations from the apparent vertical  $S^*$ -coordinates into the  $S$ -coordinates in the laboratory. That is,

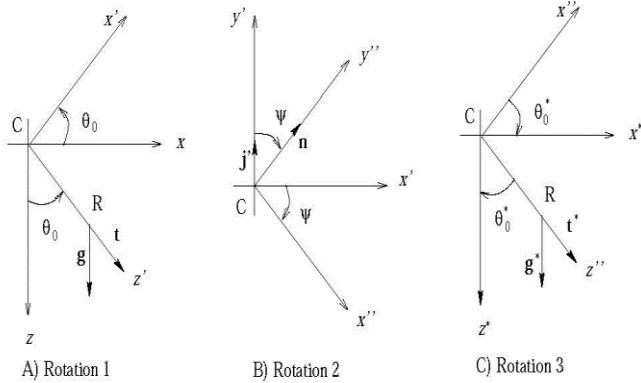


FIGURA 7. The three rotations required to pass from  $S$ -coordinates to  $S^*$ -coordinates.

$$\begin{bmatrix} x \\ y \\ z \end{bmatrix} = R \begin{bmatrix} x^* \\ y^* \\ z^* \end{bmatrix}, R = R_1^t R_2^t R_3^t, \quad (23)$$

where  $R_i^t$  denotes the transpose of matrix  $R_i$ ,  $i = 1, 2, 3$ . The individual terms of the rotation matrix  $R$  are

$$\begin{aligned} r_{11} &= \cos \theta_0 \cos \psi \cos \theta_0^* + \sin \theta_0^*, \\ r_{12} &= \cos \theta_0 \sin \psi, \\ r_{13} &= -\cos \theta_0 \cos \psi \sin \theta_0^* + \sin \theta_0 \cos \theta_0^*, \\ r_{21} &= -\sin \psi \cos \theta_0^*, \\ r_{22} &= \cos \psi, \\ r_{23} &= \sin \psi \sin \theta_0^*, \\ r_{31} &= -\sin \theta_0 \cos \psi \cos \theta_0^* + \cos \theta_0 \sin \theta_0^*, \\ r_{32} &= -\sin \theta_0 \sin \psi, \\ r_{33} &= \sin \theta_0 \cos \psi \sin \theta_0^* + \cos \theta_0 \cos \theta_0^*. \end{aligned} \quad (24)$$

For the particular case of a pendulum released from rest in the  $zx$ -plane, the generic solution in laboratory coordinates is

$$\begin{aligned} x &= r_{11}x^* + r_{13}z^*, \\ y &= r_{21}x^* + r_{23}z^*, \\ z &= r_{31}x^* + r_{33}z^*, \end{aligned} \quad (25)$$

### Example 3 Transversal force $\mathbf{F}$ .

Consider a pendulum released from rest, from the same position as in examples 1 and 2, subject to a transversal force leading to  $k_x = 0$ ,  $k_y \neq 0$ ,  $k_z = 0$ . In this case

$$\begin{aligned} g^* &= g\sqrt{1+k_y^2}, \cos \alpha = \frac{1}{\sqrt{1+k_y^2}}, \\ \cos \theta_0^* &= \frac{\cos \theta_0}{\sqrt{1+k_y^2}}, N = \frac{\sqrt{\sin^2 \theta_0 + k_y^2}}{\sqrt{1+k_y^2}}, \\ \cos \psi &= \frac{\sin \theta_0}{\sqrt{\sin^2 \theta_0 + k_y^2}}. \end{aligned} \quad (26)$$

Substituting (26) into (24) and using (25), we obtain the solution in the laboratory system:

$$x = \frac{\sqrt{1+k_y^2} \sin \theta_0}{\sqrt{\sin^2 \theta_0 + k_y^2}} L \sin \theta^*(t), \quad (27)$$

$$y = \frac{Lk_y}{\sqrt{1+k_y^2}} \left( \cos \theta^*(t) - \frac{\% \cos \theta_0}{\sqrt{\sin^2 \theta_0 + k_y^2}} \sin \theta^*(t) \right), \quad (28)$$

$$z = \frac{L}{\sqrt{1+k_y^2}} \left( \cos \theta^*(t) + \frac{\% k_y^2 \cos \theta_0}{\sqrt{\sin^2 \theta_0 + k_y^2}} \sin \theta^*(t) \right). \quad (29)$$

Fig. 8 shows the 3D-trajectories in the laboratory for  $\theta_0 = 0.1$  rad,  $L = 1$  m,  $g = 9.8 \text{ m/s}^2$  and various  $k_y$ . For  $k_y = 0$  oscillation occurs in the  $zx$ -plane, which is the usual case in the absence of force  $\mathbf{F}$ . When  $k_y$  is increased, the oscillation plane is tilted in the same direction of force  $\mathbf{F} = mA_y$  (see Fig. 8). Note that in the laboratory the trajectories are curved, although for small values of  $k_y$  the curvature is not perceptible. This is illustrated with the projections shown in Fig. 9 for larger values of  $k_y$ , also note that the amplitude of oscillation increases with  $k_y$ .

In the present example the period varies analogously to Eq. 10 for the longitudinal case. Then, a transversal force modifies all observable parameters of the pendulum: period, amplitude and plane of oscillation.

It is easy to show that the projection of the trajectory on the  $xy$ -plane is not a straight line, but a section of a rotated ellipse. Eliminating time from equations 27-28 we obtain an ellipse

$$x^2 \csc^2 \theta_0 + \left( 1 + \frac{1}{k_y^2} \right) y^2 + \frac{2 \cot \theta_0}{k_y} xy = L^2, \quad (30)$$

The intercept of this projection with the  $y$ -axis represents the displacement of the bob in the direction of  $\mathbf{F}$ :

$$y_c = \frac{Lk_y}{\sqrt{1+k_y^2}}. \quad (31)$$

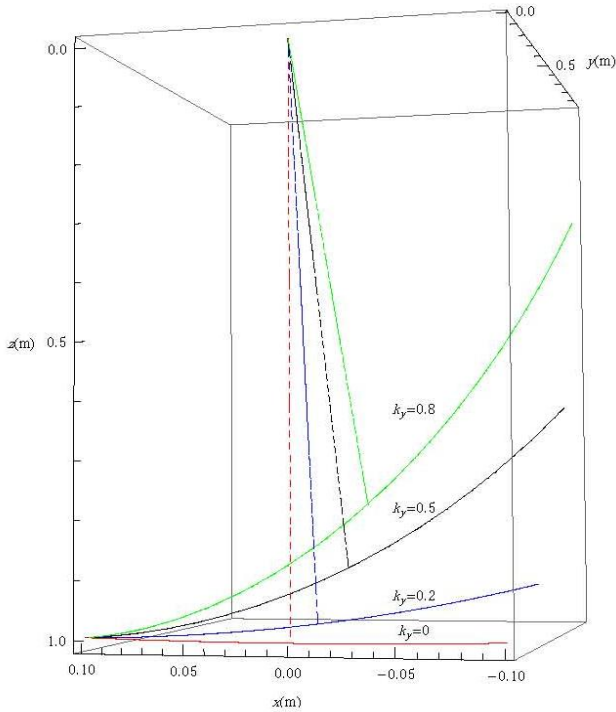


**FIGURA 8.** Trajectory in the  $xyz$ -space for different values of  $k_y$ . When  $k_y$  increases the apparent vertical (dashed lines) is tilted in the same direction as force  $mA_y$ , and the curved shape of the trajectory is manifest.

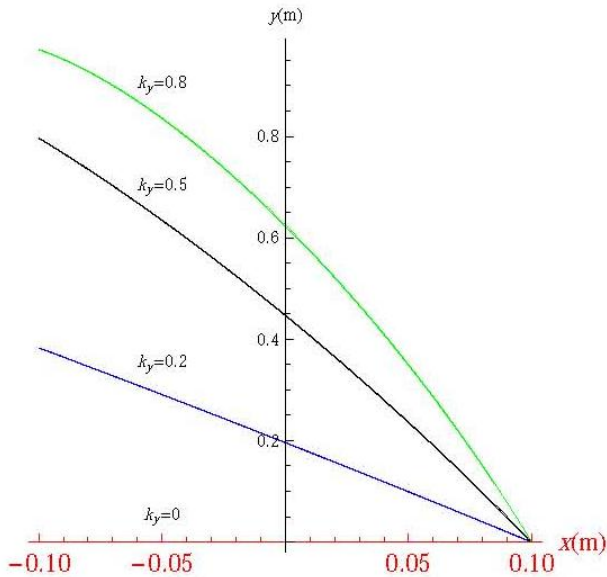


**FIGURA 9.** Projection onto the  $xy$ -plane of the trajectories plotted in Fig. 8.

## V. BEYOND THE ELEMENTARY PENDULUM

The earth is a rotating laboratory, thus leading to the well-known Foucault effect, where the plane of oscillation of the pendulum (constant in an inertial frame) rotates clockwise. There are other more subtle effects related to the initial

The method of the apparent vertical applied to pendulum dynamics conditions at the instant of release  $t = 0$ , typically from rest relative to the terrestrial laboratory. However, relative to an inertial system the tangential velocity of the center of mass of the pendulum is not the same as the velocity of the point of support, and -even more important- the derivatives of the Euler angles that represent spin around the center of mass are non-zero.

The ideal Foucault pendulum has a massive bob supported by a long wire, which is conventionally modelled by the ideal spherical pendulum discussed in the foregoing sections. Perturbations arising from the non-zero initial spin of the bob are usually neglected. This is acceptable because Foucault pendulums are usually operated subject to a periodic driving kick that keeps the bob in a given oscillation plane, and because other real life complications, like air-dragging, are not even mentioned. For the paraconical pendulum, however, non-zero initial conditions may be relevant. The effect of a force  $\mathbf{F}$  upon the Foucault pendulum may be easily calculated by just writing the solutions that are reported in the literature for the rotated system  $S^*$ , followed by a rotation back to the usual coordinates  $S$ . [14, 15, 16, 17].

Let us consider an ideal spherical pendulum released with initial velocity. In this case there is initial angular momentum and the pendulum moves in 3D. Due to the constraint  $r = L$  there are two degrees of freedom only. In spherical coordinates the relevant variables are  $\theta^*$  and  $\varphi^*$ , which satisfy the following equations (see any intermediate mechanics textbook, for instance [12], [13] or [18]),

$$\ddot{\theta}^* - \left( \frac{L_z^*}{mL^2 \sin^2 \theta^*} \right)^2 \sin \theta^* \cos \theta^* + \omega_0^{*2} \sin \theta^* = 0, \quad \dot{\varphi}^* = \frac{L_z^*}{mL^2 \sin^2 \theta^*}, \quad (32)$$

$$\dot{\varphi}^* = \frac{L_z^*}{mL^2 \sin^2 \theta^*}, \quad (33)$$

where  $L_z^*$  is angular momentum along the  $z^*$ -axis.

Eq. (32) can be integrated to obtain the usual solution for angle  $\theta^*$  in terms of the constants of motion  $E$  and  $L_z^*$

$$\dot{\theta}^{*2} = 2 \omega_0^{*2} \cos \theta^* + \frac{2E}{mL^2} - \left( \frac{L_z^*}{mL^2 \sin \theta^*} \right)^2. \quad (34)$$

Eqs. (33) and (34) formally solve the problem in the rotated coordinates  $S^*$ . In Cartesian coordinates, the trajectory of the bob in  $S^*$  is

$$x^* = L \sin \theta^* \cos \varphi^*, \quad y^* = L \sin \theta^* \sin \varphi^*, \quad z^* = L \cos \theta^*. \quad (35)$$

As before, the trajectory of the pendulum in laboratory coordinates  $S$  is easily obtained from Eqs. (35) using the rotation of Eq. (23)

### Example 4 Release with transversal velocity

In example 3 let the bob have initial transversal speed  $\dot{y}_0$

= -0.0001 m/s, which is the right order of magnitude for a paraconical pendulum of 1 meter of length released from rest in the laboratory. Numerical solution of the system of equations 33 through 35 yields the curves shown as figure 10 for the rotated coordinates  $S^*$ , where continuous curves represent  $k_y = 0.1$ , and dashed curves  $k_y = 0$ . Two trajectories are shown: the first oscillation of the pendulum between  $0 < t < \tau$  (approximately horizontal), and an oscillation 5 minutes later (i.e.  $300s < t < \tau + 300s$ ). Figure 10A shows the 3D curve, and 10B the projection on the  $x^*y^*$ -plane. Evidently, the presence of initial velocity generates ellipses with a clear precession (clockwise in this example). Figure 11 shows the trajectories in the laboratory system  $S$ , obtained from figure 10 using Eq. 23. The 3D paths are in fig. 11A, and the projections on the  $xy$ -plane are in figure 11B; note that the oscillations at  $t = 0$ , and  $t = 300s$  cannot be visually discriminated. The insets in fig. 11B show the details at the crossing of the pendulum with the  $y$ -axis, crossing that is used to observe the evolution of the minor axis of the ellipses. These variations cannot be observed by the naked eye, but are observable with laser rangefinders.

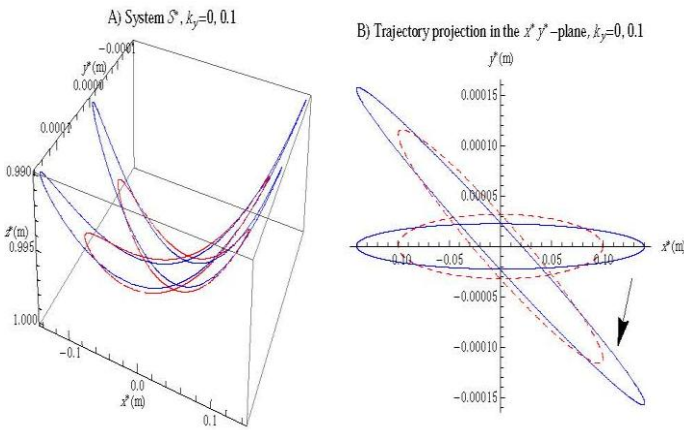


**FIGURA 10.** Trajectories in the rotated coordinates  $S^*$ , for  $k_y = 0.1$  (continuous lines) and  $k_y = 0$  (dashed curves). The first oscillation (approximately horizontal) and an oscillation 5 minutes later are shown. The arrow indicates the direction of the precession. A) Trajectories in 3D-space. B) Projection onto the  $x^*y^*$ -plane.

Paraconical pendulums are short and have a complex form, that is captured by the tensor of inertia. The point of suspension C in the Romanian pendulum moves within a small region at the bottom of a cup, [19] but in the case of Allais [2] and Goodey's pendulums the point of suspension C may wander more freely upon a horizontal plane. Paraconical pendulums are similar to spinning tops, with two differences: the center of mass of the pendulum is below the point of contact with the support, and the spin of the pendulum (i.e. rotation around its center of mass) is small. Goodey's paraconical pendulum is symmetric, so that the tensor of inertia is diagonal; but Allais and the Romanian pendulums are asymmetric, so that the tensor of inertia contains non-zero terms outside the diagonal. With the appropriate modifications, the extensive literature on tops

may be applied to the paraconical pendulum, for instance advanced texts on mechanics as [20] and [21], or the modern method of geometric algebra as revived by Hestenes, [8], [22].

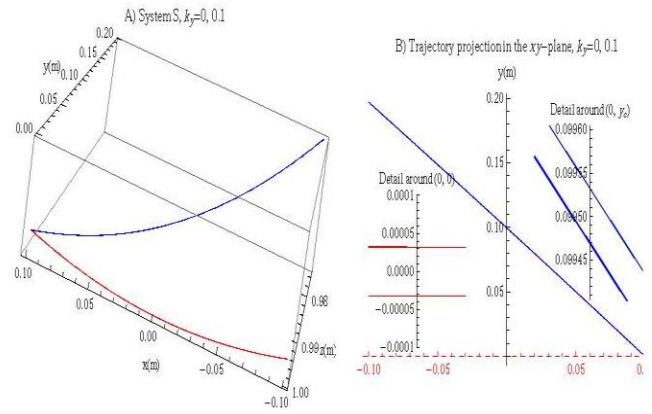


**FIGURE 11.** Same as in figure 10, but in laboratory coordinates system  $S$ . The oscillations at  $t = 0$  and  $300s$  cannot be visually discerned. A) 3D-trajectories. B) Projection onto the laboratory  $xy$ -plane. Two insets show enlarged details at the  $y$ -axis crossing.

## VI. CONCLUDING REMARKS

The paper described the method of the apparent vertical (MAV) for the solution of dynamical problems in elementary classical mechanics. The MAV amounts to a geometrical interpretation of the usual procedure of change of variables for the solution of differential equations. The method was illustrated with the dynamics of a simple pendulum  $r \rightarrow r^*$ ,  $g \rightarrow g^* = g + \mathbf{A}$ . The action of an additional force  $\mathbf{F}$  produces a change in the orientation of the plane of oscillation of the pendulum. The solution is based on a rotation of the system of coordinates so that the vertical direction coincides with the apparent acceleration of gravity  $g^*$ .

An important implication of the MAV is that problems with forces other than terrestrial gravity are reverted back to the elementary dynamical problem of a body subject only to its weight. Then all theorems related to conservation of energy and momentum in a constant gravitational field remain valid in the rotated system.

The MAV is valid for constant force  $\mathbf{F}$ , but may be applied as a first-order approximation for slowly varying forces, for instance, the gravitational effect of the sun and the moon upon the dynamics of the pendulum. The individual effect of each component of force—vertical, longitudinal and transversal to the plane of oscillation—upon amplitude, period and orientation of the oscillation plane was shown.

In the particular case of the effect due to the gravitational field of the sun and the moon, one may expect tiny variations of the amplitude, period and plane of oscillation of the pendulum in the course of a day (resembling harmonic variations over 24 hours), that can be detected if the

sensitivity of the instruments used to measure the period and the position of the pendulum is sufficient. During a solar eclipse, the period may increase or decrease, depending of the location of observation –i.e. of the relative values of the three force components produced by the combined pull of sun and moon–, and of the orientation of the plane of release of the pendulum relative to the sun and moon.

In a future paper the method will be applied to the physical paraconical pendulum, to calculate the evolution of spin and plane of precession arising from the non-zero initial conditions; of particular interest is to establish to which extent the effects discussed in the present paper may explain the variations of period, [23, 19, 24] and plane of oscillation [2] observed during solar eclipses.

## ACKNOWLEDGMENTS

The authors are indebted to two anonymous referees that provided suggestions that help improve the clarity of the presentation.

## REFERENCES

- [1] Duif, Chris P., *A review of conventional explanations of anomalous observations during solar eclipses*, arXiv:gr-qc/0408023 v2 (11 Aug 2004).
- [2] (a) Allais, Maurice. *L'Anisotropie De L'Espace*, Clément Juglar, *Mouvement du pendule paraconique et 'eclipse totale de Soleil du 30 juin 1954*, (Editorial?, Paris, 1997) p. 757 (b) M. Allais, *Compt. Rend. Acad. Sci. Paris* **245**, 2001-2003 (1957). (c) M. Allais, "Observations des mouvements du pendule paraconique," *Compt. Rend. Acad. Sci. Paris* **245**, 1697-1700 (1957).
- [3] Braginsky, V. B., Polnarev, A. G., and Thorne, K. S., *Experiments with probe masses*, *Phys. Rev. Lett.* **53** (1984), 863
- [4] van Flandern, T. and Yang, X.-S., Allais gravity and pendulum effects during solar eclipses explained, *Phys. Rev. D* **67**, 022002 (2003).
- [5] Gusev, A. V., and Vinogradov, M. P., Angular velocity of rotation of the swing plane of a spherical pendulum with anisotropic suspension, *Measurement Techniques* **36**, 1078-1082 (1993).
- [6] Yang, X.-S. and Wang, Q.S., Gravity anomaly during the Mohe total solar eclipse and new constraint on gravitational shielding parameter, *Astrophys. Space Sci.* **282**, 245 (2002).
- [7] van Ruymbeke, M., Shaoming, L., Mansinha, L. and Meurers, B., Search for the gravitational absorption effect using spring and super-conducting gravimeters during the total solar eclipse of August 11, 1999, *Bull. d'Information de Marées Terrestres (BIM)* **138**, 10967 (2003) .
- [8] Hestenes, D., *New Foundations of Classical Mechanics*,

- The method of the apparent vertical applied to pendulum dynamics* (D. Reidel Publishing Co., Dordrecht, Holland, 1986), p. 644.
- [9] Terje G. V., *An introduction to geometric algebra with an application in rigid body mechanics*, *Am. J. Phys.* **61**, 491-504 (1993).
- [10] Múnera, H. A., *The effective horizontal plane and vertical direction: Classroom demonstrations of the principle of equivalence*, accepted for publication in *The Physics Teacher* (to appear in 2010).
- [11] Brizard, A., *A primer on elliptic functions with applications in classical mechanics*, arXiv:0711.4064 (2007)
- [12] Sommerfeld, Arnold., *Mechanics-Lectures on Theoretical Physics, vol. 1*, (Academic Press, USA, 1964), p. 289.
- [13] Synge, J. L. and Griffith, B. A., *Principios de Mecánica (Translation into Spanish of Principles of Mechanics)*, 3rd. (McGraw-Hill, USA, 1965), p. 545.
- [14] Condurache, D., Martinusi, V., *Foucault pendulum-like problems: A tensorial approach*, *International Journal of Non-Linear Mechanics* **43**, 743-760 (2008).
- [15] Ivanova, E., *On use of a new method of solution of Darboux problem for solution of the problem of motion of a ball on a Routh plane*, (St. Petersburg State Technical University, Russia, 2000).
- [16] Ivanova, E., *On one approach to solving the Darboux problem*, *Mechanics of solids* **35**, 36-43 (2000).
- [17] Ivanova, E., *Exact solution of a problem of rotation of an axisymmetric rigid body in a linear viscous medium*, *Mechanics of solids* **36**, 11-24 (2001).
- [18] Corben, H. C. and Stehle, Philip., *Classical Mechanics*, 2nd. edition, (Dover, New York, 1977), p. 389.
- [19] Olenici, Dimitrie., and Olenici, Stefan, B., *Studies upon the effects of planetary alignments performed using a Romanian style paraconical pendulum at Suceava Planetarium from August 2002 to August 2003*, pp. 403-432 *Anuarul Complexului Muzeal Bucovina*, vol. XXIX-XXX-2 (2002 -2003), Suceava, Romania (2004)
- [20] Goldstein, Herbert., *Classical Mechanics*, (Addison-Wesley, USA, 1950) p. 399.
- [21] Klein, F., Sommerfeld, A., *The Theory Of The Top*, Vol. 2, (Springer, USA, 2008), (see <http://home.t01.itscom.net/allais/whiteprior>).
- [22] Snygg, J., *Expediting the spinning top problem with a small amount of Clifford algebra*, *Am. J. Phys.* **54**, 708-712 (1986).
- [23] Jeverdan, G. T., Rusu, G. I. and Antonescu, V., *Expériences à l'aide du pendule de Foucault pendant l'eclipse de Soleil du 15 février 1961*, *Science et Foi* **2**, 24-26 (1991).
- [24] Mihaila, Ieronim., Marcov, Nicolae., Pambuccian, Varujan., and Agop, Marcel., *Observation de l'effet d'Allais lors de l'eclipse de soleil du 11 août 1999*, *Proceedings of the Romanian Academy, Series A*, **4** (1), 1-5 (2003)